Effects of Vapor-Phase-Formaldehyde Treatments on Thermal Conductivity and Diffusivity of Ramie Fibers in the Range of Low Temperature

ATSUHIKO YAMANAKA,[1] MASATOSHI YOSHIKAWA,[2] SHUNZO ABE,[1] MASAYUKI TSUTSUMI,[1]
TAKESHI OOHAZAMA,[1] TOORU KITAGAWA,[1] HIROYUKI FUJISHIRO,[3] KIMIKO EMA,[4]
YOSHINOBU IZUMI,[4] SHIGEHIRO NISHIJIMA[4]

[1]Research Center, Toyobo, Co., Ltd., 2-1-1, Katata, Ohtsu, Shiga 520-0292, Japan

[2]Textiles Products Development Center, Toyobo, Co., Ltd., 50-Innai Daimon-machi Imizu-gun Toyama 939-0295, Japan

[3]Department of Materials Science and Technology, Faculty of Engineering, Iwate University, Ueda 4-3-5, Morioka 020-8551, Japan

[4]Department of Nuclear Engineering, Graduate School of Engineering, Osaka University, Yamadaoka 2-1, Suita, Osaka 565-0871, Japan

Received 24 February 2005; revised 13 June 2005; accepted 27 June 2005
DOI: 10.1002/polb.20563

ABSTRACT: To understand the influence to thermal conductivity by bridging in the polymer fibers, the thermal conductivity, and thermal diffusivity of ramie fiber and those bridged by formaldehyde (HCHO) using vapor-phase method (VP-HCHO treatment) were investigated in the lower temperature range. The thermal conductivities of ramie fiber with and without VP-HCHO treatments decreased with decreasing temperature. Thermal diffusivities of ramie fiber with and without VP-HCHO treatments were almost constant in the temperature range of 250–50 K, and increased by decreasing temperature below 50 K. Thermal conductivity and thermal diffusivity of ramie fiber decreased by VP-HCHO treatment. The crystallinities and orientation angles of ramie fibers with and without VP-HCHO treatment were measured using solid state NMR and X-ray diffraction. These were almost independent of VP-HCHO treatment. Although tensile modulus decreased slightly by VP-HCHO treatment, the decrease could not explain the decrease in thermal conductivity and diffusivity with decreasing sound velocity. The decrease of the thermal diffusivity and thermal conductivity by VP-HCHO treatment suggested the possibility of the reduction of the mean free path of phonon by HCHO in VP-HCHO treated ramie fiber. © 2005 Wiley Periodicals, Inc. J Polym Sci Part B: Polym Phys 43: 2754–2766, 2005
Keywords: thermal conductivity; thermal diffusivity; ramie; bridge

INTRODUCTION

In applications of polymeric materials, the thermal conductivity has been an important property, for example, for a cool/warm sensation for clothing fiber or wood products, or in the thermal insulation of plastics including styro-forms.[1–4] With the recent development of superconducting and electronic engineering technologies, the thermal conductivity of structural and insulating materials used as composites in cryogenic and heat-releasing materials in electrical equipment

---

Correspondence to: A. Yamanaka (E-mail: atsuhiko_yamanaka@kt.toyobo.co.jp)

Journal of Polymer Science: Part B: Polymer Physics, Vol. 43, 2754–2766 (2005)

has become more important. Furthermore, the desired features vary, depending upon the application, from insulation for use in cryostat[5] to high thermal conductivity for use in superconducting coils[6] and electronic engineering.[7] Investigation of the factors that affect the thermal conductivity of polymeric materials is essential for the development of technologies for designing polymeric materials that possess the required thermal conductivity.

From previous studies of polymer materials, it is well known that the thermal conductivity of amorphous polymers is smaller than that of metals and semiconductors.[8,9] Therefore, these have principally been used as heat insulators. However, other reports have shown that polymeric crystals possess a high thermal conductivity in the direction in which the molecular chains are covalently bonded, polyethylene crystals being an example.[10,11] The thermal conductivity of electrical insulators is considered to be attributable to phonons,[10,12] and the heat in polymers is conducted in the direction of covalently-bonded molecular chains, whereas conduction in the direction of intermolecular chains bonded by Van der Waals forces is much less. Therefore, the thermal conductivity depends on the crystallization, orientation, crystal size, and defects in the polymer crystal material. Thus, high-crystallization and high-orientation polymers exhibit high thermal conductivity.[11–16] For example, highly crystallized polymer materials, including high-strength polyethylene fiber[16–19] and high-strength polypara-phenylene-benzo-bisoxazole fiber[17] are known to possess high thermal conductivity similar to that of metals. The thermal conductivity of polymers, therefore, ranges from high to low depending on the crystal structure or morphology.

The thermal conductivity of solid, electrically insulating materials is affected by the scattering of phonons. The phonon scattering is considered to be introduced by imperfections on the surface of the material, the grain boundaries or intracrystal impurities, or interphonon dispersion in the material.[20] Therefore, in polymers, crystal or amorphous boundary, defects, the ends and entanglements of the molecular chains can scatter phonons and interfere with the thermal transmittance. In polymers, it is expected that the phonon is also scattered by impurities like the following; molecular impurities inter molecular chain, chemical branch or graft, chemical bridge points, chemical impurities copolymerized in the polymer chain, or chemical boundary in the block copolymer. Therefore, in the case of the thermal conduction of polymer fibers in the fiber direction, the mean free path of phonons is influenced not only by the crystallization or orientation, but also by the length of molecular chains and the length between the impurities mentioned above. That is to say, the mean free path of phonon is expected to depend on the concentration of chemical branch, bridge points, and interchain impurities. The changes in the mean free path of phonons result in changes in the thermal conductivity. In this report, changes in the thermal conductivity due to bridging or graft in the polymer fibers are described.

Fibers mainly made of cellulose, including ramie and cottons, are well known for being bridged with formaldehyde (HCHO),[21–28] for example, by vapor–phase-formaldehyde method (VP-HCHO treatment).[21] This technology is employed for stabilizing the conformity of cellulose fibers and is used practically in clothing materials such as wash and wear shirts.[22,26–29] There are bridge points and graft points combing cellulose chain and HCHO in the cellulose fibers with VP treatment. It is expected that the phonon is scattered at the bridge or graft points in cellulose fiber, with VP-HCHO treatment. Therefore, the mean free path of phonon in fiber direction of cellulose fiber is expected to reduce by scattering of phonon at bridge or graft points combined with HCHO. That is to say, thermal conductivity and diffusivity are considered to decrease by VP-HCHO treatment. In this paper, we report the effect of VP-HCHO treatment on the thermal conductivity and diffusivity of ramie fiber in the range of low temperature.

EXPERIMENTAL

Sample

In this work, thermal conductivity and diffusivity of raw and VP-HCHO-treated ramie were measured in the range of low temperature. The sample preparations are described in the following section.

Ramie Fibers

The ramie fiber samples used in this work were made in China. The ramie fiber were scoured and bleached. The density and fineness of ramie fibers were 1.54 and 4.3 dtex, respectively.

The VP-HCHO-Treated Ramie Fibers

Two kinds of ramie fibers were prepared by VP-HCHO treatment.[21] In the VP-HCHO treatment, the ramie fibers were washed by steam and were exhausted in vacuum to remove free HCHO. Details of VP-HCHO treatment are described elsewhere.[21] The concentrations of bound HCHO of the two kinds of VP-HCHO-treated ramie fibers were 0.7% and 1.6%, respectively. These are hereinafter abbreviated to VP (0.7) and VP (1.6). The density of ramie fibers with VP-HCHO treatment was 1.55.

The concentrations of bound HCHO were measured by iodometric titration of HCHO with hydrolysis of VP-HCHO-treated ramie fibers. Details of measurements of concentration of bound HCHO are described elsewhere.[21] The densities of ramie fibers with and without VP-HCHO treatment were measured by pycnometer after drying at 383 K × 8 h.

Measurements

Thermal conductivity and diffusivity depend on not only bridge or graft points but also the crystallinity and orientation angle of crystal.[11–16] To investigate the relative changes of the crystallinity and orientation angle by VP-HCHO treatment, the crystallinities and orientation angles of ramie fibers with and without VP-HCHO treatment were measured by solid state high resolution NMR and X-ray diffraction, respectively. The tensile moduli of the fibers were measured for relative comparison of sound velocities of the ramie fibers with and without VP-HCHO treatment. In this section, the measurements of crystallinities, orientation angles, tensile modulus are described, and the measurements of thermal conductivity and diffusivity are described in the following section.

Thermal Conductivity

Thermal conductivity (κ) was measured by a steady-state heat flow method.[17,30] The measurements of κ were carried out on the automated measuring system with thermal controller of a Gifford–MacMahon (GM) cycle helium refrigerator as a cryostat.[30]

The fiber samples were stored in a desiccator for more than three weeks. The fiber samples were prepared by bundling about 400–8500 monofilaments with length of 25 mm. Both ends of the fiber bundle were fixed by adhesive Stycast GT. One end of the bundle was attached to the cold stage of a GM refrigerator by mechanical pressing using indium metal and the adhesive Stycast GT. A small resistance heater (1 kΩ) was adhered to the other end of the bundle using GE7031 varnish. The intermediate positions where thermocouples were contacted were bound by fine (0.1 mm) Cu wire. Au (Fe at 0.07%)-chromel thermocouples were used as thermometers, which were adhered by GE7031 varnish. The sample space was evacuated to below 10^{-3} Pa by an oil diffusion pump for heat insulation. Before the measurements, the sample space was kept at high vacuum below 10^{-3} Pa for 24 h to dry up the sample.

The automated measuring system of κ was operated in the temperature range of 10–250 K. The κ was estimated by the relation $\kappa(\mathrm{mW/cm\ K}) = (Q/\Delta T)(L/S)$, where Q is the heat flow per second, ΔT is the temperature difference between thermometers, L is the distance between the thermometers, and S is the cross section of the bundle. Details of the determination of κ are described elsewhere.[17,18]

Thermal Diffusivity

Thermal diffusivity (λ) was measured by non-steady-state heating method.[17,18,30] The measurements of λ were carried out on the same system as that for measurements of thermal conductivity. In this method, time evolutions of temperature at two measurement points, the intermediate positions between the cold head and 1 kΩ heater, were recorded after applying heat pulse from the heater, and the measured temperature change was compared once for various λ values. The fiber samples were stored in a desiccator for more than a week. The fiber samples were prepared and were set in the sample space by the same way as that for the measurements of thermal conductivity mentioned above. The sample space was evacuated to below 10^{-3} Pa by an oil diffusion pump for heat insulation and was kept for 24 h before the measurements for drying up the sample. The automated measuring system of λ was operated in the temperature range of 10–250 K. Details of the determination of λ are described elsewhere.[17,18,30]

Water Contents

To measure the water contents of the samples used in the measurements of thermal conductivity and thermal diffusivity, the samples were stored at high vacuum below 10^{-3} Pa for 24 h in the sample space in the same way for measurement of thermal conductivity. The weights of those samples were defined as W. The dried samples were obtained by drying them at 383 K for 8 h in vacuum at 1 Pa as described elsewhere.[31,32] The weights of dried samples were defined as W_d. The water contents of those samples were estimated by the difference between W and W_d.

Crystallinity

It is known that the chemical shifts of cellulose in solid state ^{13}C NMR spectra are different by the difference in crystal structure, for example cellulose I and II.[33–35] It is also known that the resonance lines of C4 and C6 carbons split into crystal and amorphous components in solid state ^{13}C NMR spectra of cellulose.[33,34,36,37] The changes in crystal structures and crystallinities of cellulose fibers by mercerization or liquid ammonia treatment were studied with solid state NMR.[38,39] In this work, the changes in crystal structure and crystallinity by VP-HCHO treatment are investigated by solid state NMR.

Solid state NMR measurements were carried out on Brucker Avance 300 (^{13}C, 75.5 MHz). NMR spectra were measured by cross-polarization (CP), high power proton decoupling, magic angle spinning (MAS) methods. Pulse width was 4 μs and magic angle spinning rate was 4.5 kHz.

Orientation Angle

Orientation angle of crystallic phase to fiber axis was estimated by X-ray diffraction. The samples were prepared in the form of a bundle of about 30 filaments in parallel and they were fixed at both ends. Rigaku RU-200 (40 kV × 100 mA) was used with X-ray diffraction on Ni-filtered Cu Kα (λ = 0.1548 nm). The intensity distribution of (002) diffraction spot was used for estimating orientation angles.

Tensile Modulus

The tensile test of a single fiber was carried out on small tensilon Toyo Sokki UTM-II. The span length was 10 mm and the crosshead speed was 10 mm/min.

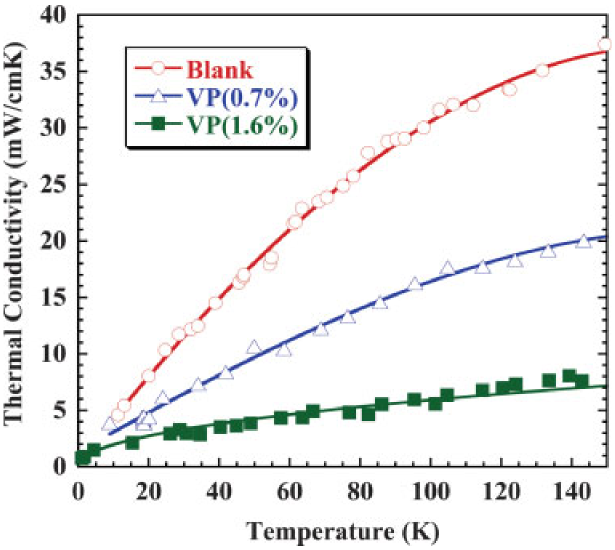

Figure 1. Temperature-dependence of thermal conductivities of ramie fibers with VP-HCHO treatment. [Color figure can be viewed in the online issue, which is available at www.interscience.wiley.com.]

RESULTS AND DISCUSSION

The Change in Thermal Conductivity of Ramie Fiber by VP-HCHO Treatment

The temperature dependence of thermal conductivity of ramie fibers with and without VP-HCHO treatments in fiber direction from 10 to 150 K are shown in Figure 1. The number of filaments used in these measurements are more than 6000. Thermal conductivities of all samples decrease with decreasing temperature. Those ramie fibers are electrical insulators. Therefore, it is considered that thermal conduction of ramie fibers is caused by phonon conduction like most of the polymer materials.

As for the effect of VP-HCHO treatment, thermal conductivity of ramie fiber decreases. The thermal conductivity of ramie fiber decreases to about 50% and 20–25% by the VP-HCHO treatment for the concentration of 0.7% and 1.6% HCHO, respectively. To clear the changes in the thermal conductivity by VP-HCHO treatment, the relation between the thermal conductivity at 120, 100, 80, and 60 K and the concentration of the bound HCHO in the ramie fibers are shown in Table 1. As shown in Table 1, the thermal conductivity decreases by bridge of HCHO at every temperature. The concentration of bound HCHO is higher; the thermal conductivity is lower.

This decrease in thermal conductivity is inferred to be caused by the change in several

Table 1. Thermal Conductivity and Thermal Diffusivity of Ramie Fibers With and Without VP-HVHO Treatment

Sample	Bound HCHO (%)	Thermal Conductivity (mW/cm K)				Thermal Diffusivity at 240 K (mm^2/s)
		120 K	100 K	80 K	60 K	
Ramie	0	34.0	30.5	26.3	21.0	0.94
VP (0.7)	0.7	18.4	16.5	14.0	11.3	0.42
VP (1.6)	1.6	7.0	6.0	5.5	4.8	0.23

properties, such as radiation effect, water content, crystallinity, crystal structure, orientation degree, and mean free path of phonon by bridging or graft reaction with VP-HCHO treatment. The changes in these properties are investigated in the following section.

Radiation Effect in the Measurement of Thermal Conductivity

Temperature dependence of thermal conductivity of various number of ramie fibers in the fiber direction from 10 to 250 K are shown in Figure 2. In the temperature range below 100 K, the observed thermal conductivities are independent of the number of filaments and the slopes of the curves decrease with increasing temperature. On the other hand, the observed thermal conductivities depend on the number of filaments, and the slopes of the curves increase with increasing temperature in higher temperature range. The observed thermal conductivity is higher with decreasing the number of filaments in higher temperature range. The dependence of observed thermal conductivity on the number of filaments in the higher temperature range is inferred to be caused by radiation effect. In the temperature range over 200 K, the observed thermal conductivity show the behavior influenced by radiation effect even if the number of filaments are more than 5000. Therefore, it is difficult to observe the thermal conductivity in the higher temperature range more than 200 K. On the other hand, the radiation effect can be neglected in low temperature range in the case where the number of filaments is more than 6000.

The radiation effect of thermal conductivity also depends on the side shape of filament. The photographs of ramie fibers by scanning electron microscope are shown in Figure 3. The shape of the side view does not change distinctly by VP-HCHO treatment in the case of bound HCHO below 1.6%. Therefore, the radiation effect does not change by change in shape, with VP-HCHO treatment. The ramie fibers with VP-HCHO treatment show the same behavior of filament number dependence. Therefore, the radiation effect can be neglected in the measurements of thermal conductivity in the temperature range below 150 K, with more than 6000 filaments for the discussion of the effect of VP-HCHO treatment on the thermal conductivity.

Water Content

The water contents of ramie fibers, with and without VP-HCHO treatment, used in this work are smaller than 0.1%. After the measurements of thermal conductivity, the ramie sample was dried at 383 K for 8 h in vacuum at 1 Pa and thermal conductivity was measured again. The temperature dependence of thermal conductiv-

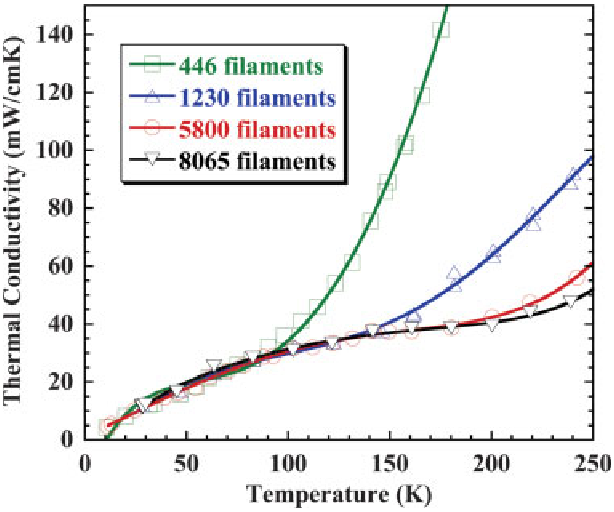

Figure 2. Temperature-dependence of thermal conductivity of ramie fibers with various number of filaments. [Color figure can be viewed in the online issue, which is available at www.interscience.wiley.com.]

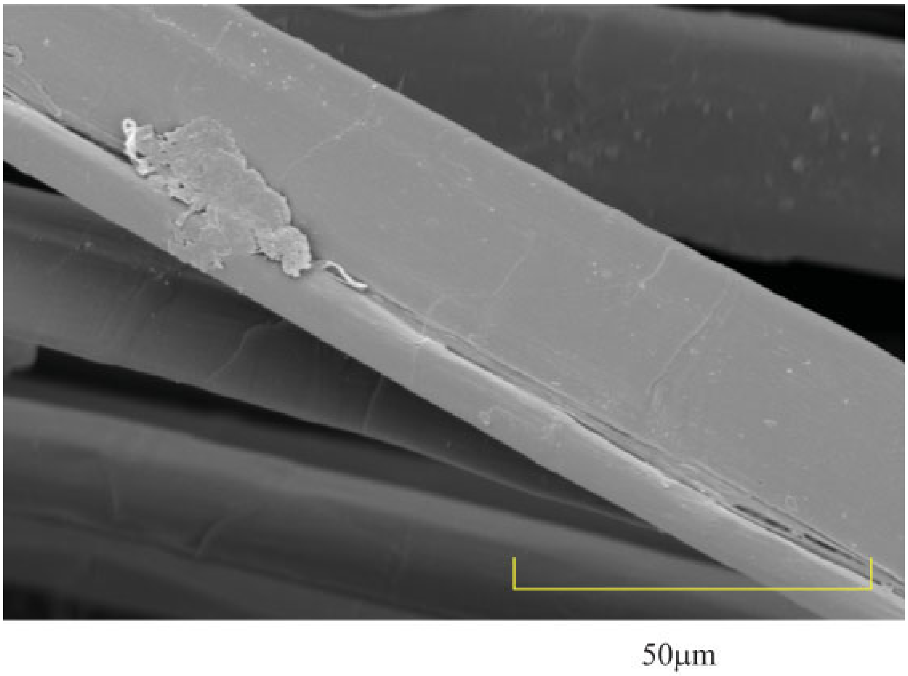

Ramie (Blank)

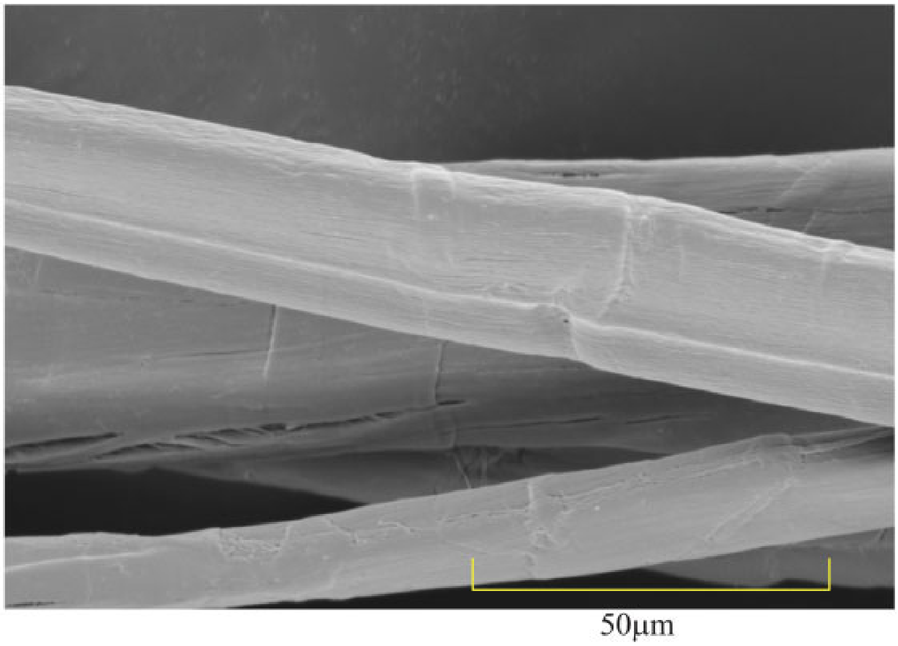

VP(1.6)

Figure 3. Side view of ramie fibers with and without VP-HCHO treatment by scanning electron microscope. [Color figure can be viewed in the online issue, which is available at www.interscience.wiley.com.]

ities of ramie fibers before and after dry treatment are shown in Figure 4. This figure shows that thermal conductivity does not change by dry treatment compared with VP-HCHO treatment. Therefore, the influence of thermal conductivity of 0.1% water is neglected in this article.

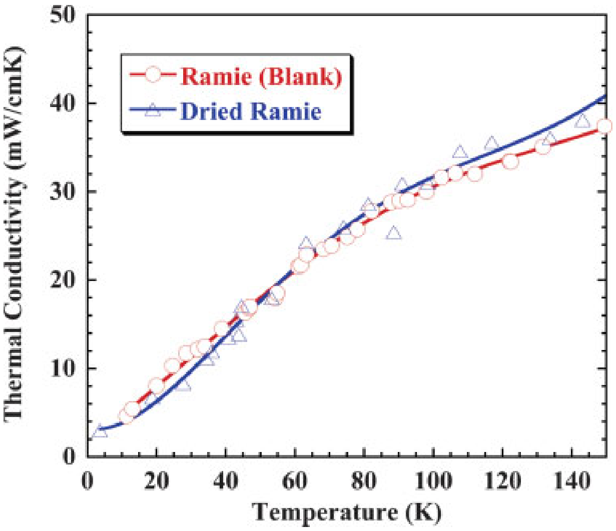

Figure 4. Temperature-dependence of thermal conductivity of ramie fibers with and without dry treatment. [Color figure can be viewed in the online issue, which is available at www.interscience.wiley.com.]

Thermal conductivity depends on heat capacity, density, and thermal diffusivity as shown in the follwing formula (1).[17,18]

$$\kappa = C_p \rho \lambda \tag{1}$$

In this formula, the parameters are defined as follows: κ, thermal conductivity in the fiber direction; C_p, heat capacity at constant pressure; ρ, density of ramie fiber; λ, thermal diffusivity in the fiber direction. It is known that heat capacity of cellulose depends on water contents.[40] The change in heat capacity by 0.1% water is estimated to be about 0.25%, according to the relation[40] between heat capacity and water contents. From this formula, the influence to thermal conductivity with the change in heat capacity induced by 0.1% water is about 0.25% and it can be neglected in this work. Therefore, it is also considered that thermal diffusivity does not change by 0.1% water according to formula (1).

Crystallinity

^{13}C-CP-MAS solid state NMR spectra of ramie fibers with and without VP-HCHO treatments are shown in Figure 5. The assignments of resonance lines are shown in this figure. It is known that the crystal structure of ramie is Cellulose I type.[34,41–43] All the NMR spectra show same peak shape and chemical shifts of the crystal structure of Cellulose I type.[34]

The resonance lines of C4 and C6 carbons split into crystal and amorphous components.[33,34,36] The peaks of crystal are sharp and those of amorphous are broad. Because the peak splitting of C4 resonance is larger than that of C6 resonance, C4 resonance peaks are used for estimation of crystallinity. The C4 peak separations of ramie fibers with and without VP-HCHO treatment are shown in Figure 6. The peak shape and chemical shifts do not change by bridge with HCHO (VP-HCHO treatment). It is known that a linear relationship exists between the mass fraction of the C4 crystal component peak in solid state NMR and the crystallinity determined by X-ray analysis.[34,36,44] The crystallinities of those ramie fibers estimated by peak separation are shown in Table 2. Although the crystallinity of ramie fiber increases slightly by VP-HCHO treatment, this change is not so large compared with that of thermal conductivity. Therefore it is expected that the thermal conductivity of ramie fiber is not much influenced by the relative change in crystallinity with VP-HCHO treatment.

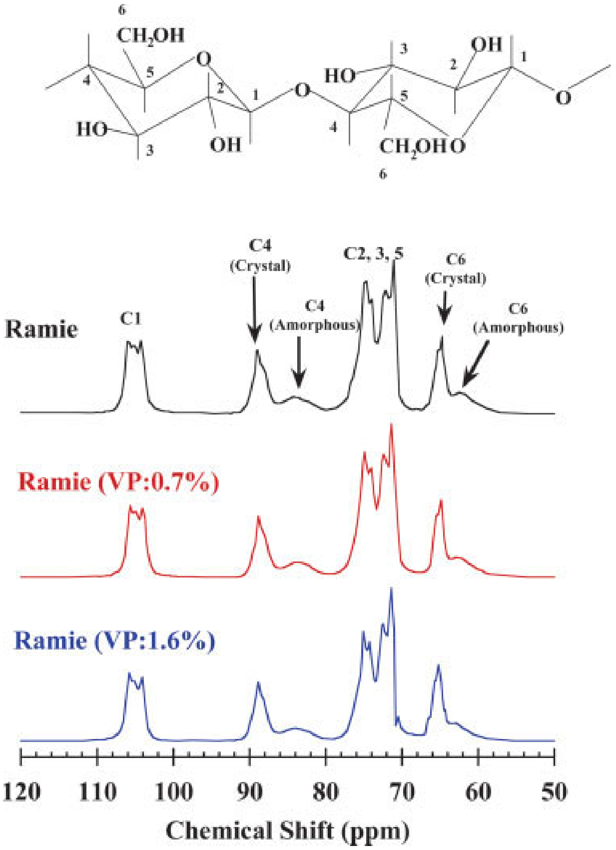

Figure 5. ^{13}C-CP-MAS solid state high resolution NMR spectra of VP-HCHO-treated ramie fibers. [Color figure can be viewed in the online issue, which is available at www.interscience.wiley.com.]

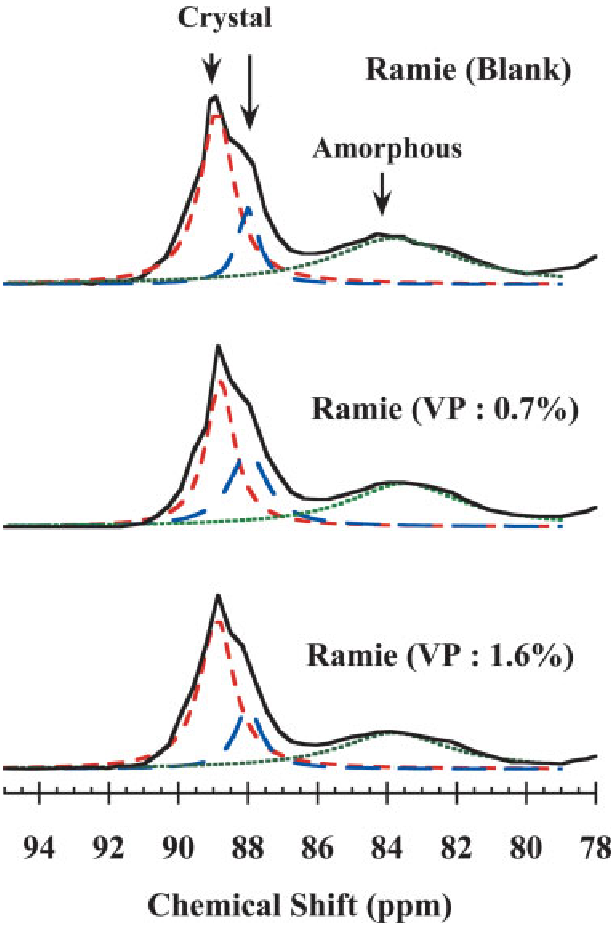

Figure 6. Line-shape analysis for C4 peaks of ramie cellulose with VP-HCHO treatment in ^{13}C-CP-MAS solid state NMR spectra. A solid line indicates observed curve, and broken lines indicate the estimated curves of crystal components and amorphous component. [Color figure can be viewed in the online issue, which is available at www.interscience.wiley.com.]

The absolute values of crystallinity estimated by solid state NMR are a little different from those estimated by X-ray.[34,44] Therefore, other measurements will be necessary for more detailed discussion about absolute crystallinity. In the following section, the orientation angles of ramie fibers with and without VP-HCHO treatments are reported.

Orientation Angle of Crystal Region

An X-ray diffraction photograph of ramie fiber is shown in Figure 7. The orientation angles of crystals were estimated by azimuthal intensity distribution of the (002) diffraction spot. X-ray diffraction profiles of (002) spot of the ramie fibers are shown in Figure 8. The half-width of diffraction peak changes not much by VP-HCHO treatments. The orientation angles are estimated by the half-width of diffraction peak and the orientation degrees are estimated by using orientation angles in the following formula (2).[24,45]

$$\phi = [(180 - \beta)/180] \times 100 \qquad (2)$$

In this formula, (2) ϕ is defined as orientation degree and β as the orientation angle.

The orientation angles and orientation degrees of ramie fibers with and without VP-HCHO treatment are shown in Table 2. It is shown that the orientation angle and the orientation degree do not change by VP-HCHO treatment in the case of bound HCHO below 1.6%.

As mentioned above, effect of radiation and water content to the change in thermal conductivity can be neglected, and the crystallinity and orientation degree of crystal do not change distinctly by VP-HCHO treatment.

Therefore, the decreasing of thermal conductivity by VP-HCHO treatment is inferred to be caused by the other changes induced by bridge or graft points. From formula (1), thermal conductivity depends on density, heat capacity, and thermal diffusivity. The density changes in less than 1% by VP-HCHO treatment. Therefore, the change in density does not contribute to the decrease of thermal conductivity by VP-HCHO treatment. The change in thermal diffusivity by

Table 2. Crystallinity and Orientation Degree of the Ramie Fibers With and Without VP-HCHO Treatment

Sample	Bound HCHO (%)	Crystallinity (%)	Orientation Angle (deg)	Orientation Degree (%)
Ramie	0	56	12.7	92.9
VP (0.7)	0.7	58	11.0	93.8
VP (1.6)	1.6	62	11.8	93.4

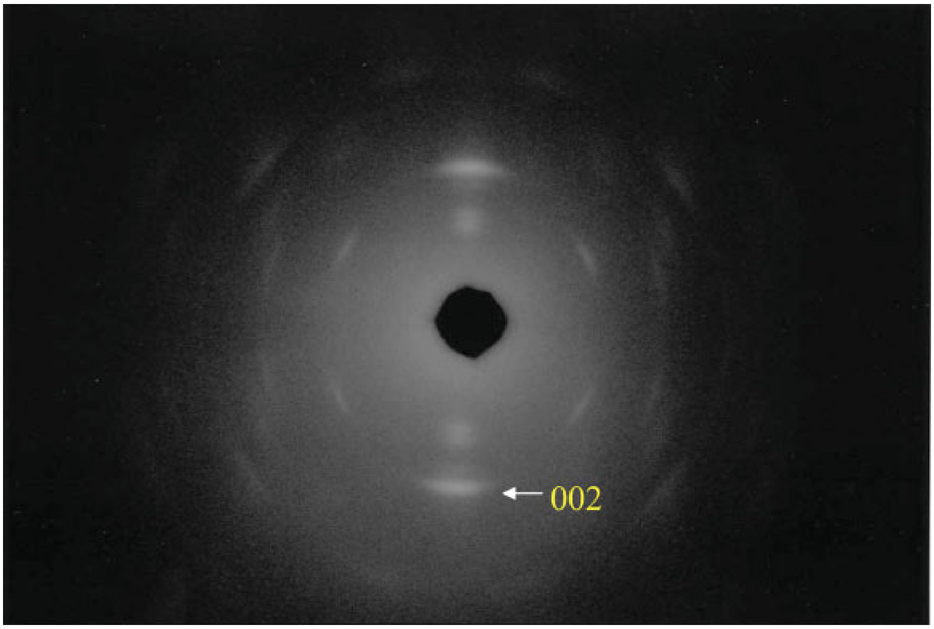

Figure 7. X-ray diffraction photograph of ramie fiber. [Color figure can be viewed in the online issue, which is available at www.interscience.wiley.com.]

VP-HCHO treatment is investigated in the following section.

The Change in Thermal Diffusivity by VP-HCHO Treatment

Temperature dependence of thermal diffusivity of ramie fibers with VP-HCHO treatment in the fiber direction is shown in Figure 9. The thermal diffusivities of all ramie fibers show almost constant values in the temperature range of 250 to 50 K and increases when temperature decreases below 50 K. As for effect of VP-HCHO treatment, the thermal diffusivity decreases distinctly in the range of all temperatures. The relation between the concentration of bound HCHO and thermal diffusivity at 240 K is shown in Table 1. Thermal diffusivity at 240 K decreases to about 45 and 25% by VP-HCHO treatment for the concentration of 0.7% and 1.6% HCHO, respectively. The decrease in thermal diffusivity agrees with that of thermal conductivity by increasing bound HCHO. Therefore, the decreasing of thermal diffusivity is one of the causes for the decreasing thermal conductivity of ramie fibers by VP-HCHO treatment. The cause of decreasing thermal diffusivity by VP-HCHO treatment, such as radiation effect and the graft or bridge points, is investigated here.

For investigation of the radiation effect in the measurements of thermal diffusivity, the temperature dependence of thermal diffusivities of ramie fibers are compared with the different number of filaments in Figure 10. The behavior of thermal diffusivity is almost independent of the number of measuring filaments. In this method, thermal diffusivity is estimated by time-depend-

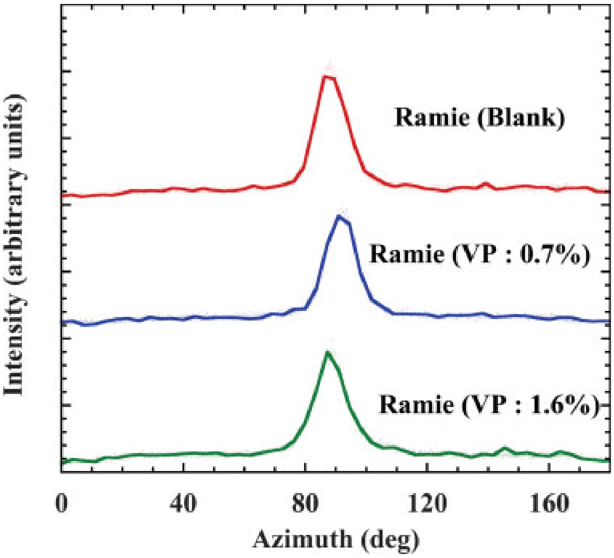

Figure 8. X-ray diffraction profile of ramie fibers with VP-HCHO treatment. [Color figure can be viewed in the online issue, which is available at www.interscience.wiley.com.]

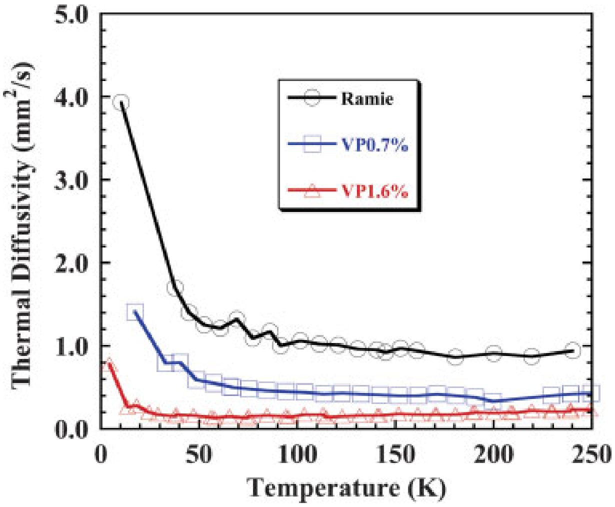

Figure 9. Temperature-dependence of thermal diffusivity of ramie fibers with VP-HCHO treatment. [Color figure can be viewed in the online issue, which is available at www.interscience.wiley.com.]

ence of temperature at two measurement points and heat flow is not used.[30] This is a different point from the measurements of thermal conductivity, although thermal diffusivity and conductivity are measured by same system. Therefore, the radiation effect to thermal diffusivity is much smaller than that to thermal conductivity, although it is not equal to 0. Therefore, the radiation effect is neglected compared with the change in thermal diffusivity by VP-HCHO treatment. This result shows that the thermal diffusivity decreases by the HCHO in the ramie fibers.

It is considered that HCHO molecules exist in the ramie fiber in the following four types; free molecule, graft combined with cellulose chain, interchain bridge, and intrachain bridge. In the four types of HCHO, it is considered that the free HCHO molecules exist in little, because the ramie fibers were washed by steam and were exhausted in vacuum to remove free HCHO, as described in the experimental section.[21] The ramie fibers treated with similar VP-HCHO method show the stability of conformity for wash and wear shirts.[22,29] Therefore, it is considered that some of the HCHO molecules exist as the interchain bridge. The average degree of polymerization of HCHO in VP-HCHO treatment fiber is reported to be 1.7.[46] It is also reported that HCHO is mostly combined at C6 carbon with cellulose.[47] Although, it is difficult to distinct the four type HCHO molecules by the iodometric titration method, it is inferred that most of the HCHO molecules exist as graft, inter-, and intra-chain bridge.

The thermal diffusivity depends on sound velocity and mean free path of phonon as shown in the following formula (3).[17,18]

$$\lambda = (1/3)vl \tag{3}$$

In this formula, the parameters are defined as follows; λ, thermal diffusivity in the fiber direction; v, sound velocity in the fiber direction; l, mean free path of phonon in the fiber direction.

The sound velocity in the fiber direction is estimated by using the tensile modulus and density in the following formula (4).

$$v = (E/\rho)^{1/2} \tag{4}$$

In this formula, v is defined as sound velocity, E as tensile modulus, and ρ as density of ramie. To discuss the cause of decreasing thermal diffusivity, the possibility of the relative change in sound velocity is discussed by tensile modulus.

The tensile modulus at room temperature in fiber direction of ramie fiber, VP (0.7) and VP (1.6) are 61, 49, and 52 GPa, respectively. It is reported that the tensile modulus increases slightly by VP-HCHO treatment in the same way after drawing in the water.[24] In this case, the tensile modulus slightly decreases by VP-HCHO treatment, in spite of the crystallinity and crystal orientation independence. The two reasons are considered as following: (1) The disordered

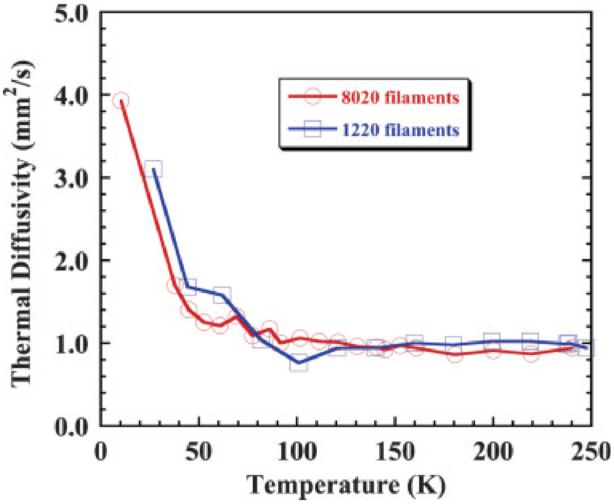

Figure 10. Temperature-dependence of thermal diffusivity of ramie fibers with various number of filaments. [Color figure can be viewed in the online issue, which is available at www.interscience.wiley.com.]

chains fixed by bridged HCHO do not contribute to tensile modulus. Those samples with VP-HCHO treatment became brittle and hard. (2) The orientation degree of molecular chain in amorphous region decreases by VP-HCHO treatment. The opposite case is reported that the tensile modulus of ramie fiber increased by the orientation of amorphous region.[24] The decreasing orientation degree of amorphous region is able to induce the decreasing sound velocity and mean free path of phonon.

The density of those samples is 1.54 and 1.55. The sound velocities of ramie, VP (0.7), and VP (1.6) at room temperature are estimated as 6400, 5700, and 5900 m/s by the substitution of the numerical values of E and ρ into the formula (4). The sound velocity estimated by tensile modulus slightly decreases by VP-HCHO treatment, although the decreasing rate is smaller than that of thermal diffusivity.

It is known that sound velocity of polymeric materials depends on temperature.[48] On the other hand, the thermal diffusivities of those ramie fibers show almost constant value in the temperature range of 50–250 K. Therefore, the thermal diffusivities of the ramie fibers at room temperature are expected to be almost equal to those at 240 K. The tensile modulus does not decrease, for explaining the decrease of thermal diffusivity by decreasing sound velocity.

Crystal region and amorphous region are mixed in the ramie fiber used in this work. The mean free path of phonon in crystal region and that in amorphous region are different. Therefore, it is difficult to discuss the absolute value of phonon mean free path in the crystal and amorphous region in this work. Therefore, the relative change in average behavior of phonon mean free path in the mixture of crystal and amorphous by VP-HCHO treatment is discussed in this work. The mean free path of phonon in the ramie fibers with VP-HCHO treatment can be compared with that in blank ramie fiber relatively by using formula (3) and the sound velocity estimated by formula (4) in the assumption that thermal diffusivities at room temperature are equal to those at 240 K. The estimated mean free path of phonon decreases with VP-HCHO treatment to 52 and 27% in the case of VP (0.7) and VP (1.6), respectively.

It is considered that all of the four types HCHO—free molecule, graft combined with cellulose chain, interchain bridge, and intrachain bridge—scatter the phonon, although the probabilities are different. That is to say, it is considered that the mean free path of phonon reduces by the HCHO, such as the graft or bridge points in the VP-HCHO treated ramie fibers. It is also considered that the decrease of orientation in the amorphous region by bridge points reduces the mean free path of phonon as mentioned above.

The probability of existence of HCHO in crystal region is considered to be different from that in amorphous region. It is considered that HCHO molecules in crystal region contribute effectively to decreasing thermal diffusivity. For more quantitative discussion, the more detailed discussion including structural analysis will be necessary.

The decreasing of thermal diffusivity of ramie fiber by VP-HCHO treatment is inferred to be caused by the reduction of the mean free path of phonons by HCHO. This result is based on some assumptions. Therefore, the direct measurements of temperature-dependence of sound velocity are necessary for detail discussion of mean free path.

Heat Capacity

From formula (1), thermal conductivity depends on not only thermal diffusivity but also heat capacity. It is known that heat capacity of cellulose depends on crystallinity.[49] But in this case, the change in heat capacity by crystallinity does not contribute to the decrease in thermal conductivity. Heat capacity is able to change by change in molecular motion induced by bridge or graft points with VP-HCHO treatment.

The observed thermal conductivities and thermal diffusivities have the experimental error of about 10% as shown in Figures 4, 9, and 10. Although the errors are smaller than the change by VP-HCHO treatment, the quantitative discussion of heat capacities is difficult by the estimation from formula (1) in this work. Therefore, it will be necessary to investigate the heat capacity independently to understand the decreasing thermal conductivity by VP-HCHO treatment.

CONCLUSIONS

Thermal conductivity and thermal diffusivity were measured by steady-state heat flow method and non-steady-state heating method for ramie fiber and those treated with formaldehyde (HCHO) by VP-HCHO treatment, with concentrations of bound formaldehyde of 0.7% and 1.6%

(VP (0.7) and VP (1.6)). The following conclusions were drawn:

1. The thermal conductivities of ramie fibers with and without VP-HCHO treatments decreased with decreasing temperature.
2. Thermal conductivity and diffusivity decreased to about 50% and 20–25% by VP-HCHO treatment in the case of VP (0.7) and VP (1.6), respectively.
3. The crystallinity and orientation degree of ramie fiber did not decrease by VP-HCHO treatment.
4. Thermal diffusivities of ramie fiber and those with VP-HCHO treatments were almost constant in the temperature range of 250–50 K, and increased by decreasing temperature below 50 K.
5. The decrease of thermal diffusivity by VP-HCHO treatment could not be explained by change in tensile modulus, although it decreased slightly by VP-HCHO. Those results suggested the possibility of the reduction of mean free path of phonon by HCHO.

As mentioned above, the thermal conductivity and thermal diffusivity decrease by bridge or graft with formaldehyde, although the crystallinty and orientation degree do not decrease. Those results suggest that thermal conductivity of polymer material could be controlled by bridge or graft structure.

Many thanks are due to Mr. Atsushi Hamai, the Fiber Business Unit, Toyobo, and the Research and Development Center for obtaining ramie samples and VP-HCHO treatment. Our gratitude is also expressed to Professor Dr. Fumitaka Horii, Kyoto University, and Dr. Seichi Ochi, Research and Development Department, Toyobo, Professor Dr. Masao Murano, Saga University and Dr. Atsushi Kaji as well as Dr. Yuji Shimizu, Toyobo, for their valuable advice and references with respect to cellulose and its structural analysis. Thanks are also due to Dr. Hiroshige Sugiyama and Dr. Sonoko Ishimaru, Toyobo for their advice and references on the engineering applications of thermal conductivity. We express our appreciation to Ms. Sayuri Nagao and Ms. Chie Sawa, Toyobo, and Mr. N. Nakajima, JEMS, who were very helpful with the experiments. We would also like to thank Professor Dr. Manabu Ikebe, Iwate University, Dr. Hiroshi Hirahata, Dr. Yukihiro Nomura and the members of their group, Toyobo Functional Fiber Group, as well as Mr. Takayuki Matsui, Manager, and Mr. Tokuichi Maeda and other members of the Toyobo Dyneema Division in addition to Dr. Takaharu Ichiryu, Zylon Business Unit, and Dr. Keiji Yukimatsu, President of Nippon Dyneema for their support.

REFERENCES AND NOTES

1. Yoneda, M.; Kawabata, S. J Text Machinery S Jpn 1981, 34, 183.
2. Yoneda, M. J Text Machinery S Jpn 1982, 35, 365.
3. Kawabata, S. J Text Machinery S Jpn 1984, 37, 131.
4. Nishijima, S.; Okada, T.; Niihara, K. Key Eng Mater 1999, 161–163, 535.
5. Hand Book of Superconductivity and Cryogenic Engineering; Cryogenic Association of Japan: Oumusha, Japan, 1993.
6. Takao, T.; Kawasaki, A.; Yamaguchi, M.; Yamamoto, H.; Niiro, A.; Nakamura, K.; Yamanaka, A. Proc of ASC 2002; IEEE Trans Appl Superconductivity 2003, 13, 1776.
7. Agari, Y.; Kamiyama, T. Plastics 2003, 54, 49.
8. Bhowmick, T.; Pattanayak, S. Cryogenics 1990, 30, 116.
9. Jackel, M.; Muller, M.; Claverie, A. L.; Arndt, K. F. Cryogenics 1991, 31, 228.
10. Choy, C. L.; Wong, S. P.; Young, K. J Polym Sci, Polym. Phys. Ed 1985, 23, 1495.
11. Choy, C. L.; Luk, W. H.; Chen, F. C. Polymer 1978, 19, 155.
12. Mergenthaler, D. B.; Pietralla, M.; Roy, S.; Killian, H. G. Macromolecules 1992, 25, 3500.
13. Burgress, S.; Greig, D. J Phys C: Solid State Phys 1975, 8, 1637.
14. Gibson, A. G.; Greig, D.; Sahota, M.; Ward, I. M.; Choy, C. L. J Polym Sci: Polym Lett Ed 1977, 15, 183.
15. Choy, C. L. Polymer 1977, 18, 984.
16. Choy, C. L.; Leung, W. P. J Polym Sci: Polym Phys Ed 1983, 21, 1243.
17. Fujishiro, H.; Ikebe, M.; Kashima, T.; Yamanaka, A. Jpn J Appl Phys 1997, 36, 5633.
18. Fujishiro, H.; Ikebe, M.; Kashima, T.; Yamanaka, A. Jpn J Appl Phys 1998, 37 1994.
19. Yamanaka, A.; Fujishiro, H.; Kashima, T.; Kitagawa, T.; Ema, K.; Izumi, Y.; Nishijima, S. J Polym Sci B: Polym Phys 2005, 43, 1495.
20. Kittel, C. Introduction to Solid State Physics; Academic Press: New York, 1974.
21. Abe, S.; Ohta, S.; Yoshikawa, M. J Text Machinery S Jpn 1997, 50, 124.
22. Abe, S.; Ohta, S.; Yoshikawa, M.; Tsutsumi, M. J Text Machinery S Jpn 1997, 50, 139.
23. Abe, S.; Ohta, S.; Yoshikawa, M.; Tsutsumi, M. J Text Machinery S Jpn 1999, 52, 29.
24. Abe, S.; Tsutsumi, M.; Yoshikawa, M.; Sakaguchi, Y. J Text Machinery S Jpn 2000, 53, 1.

25. Abe, S.; Yoshikawa, M.; Shimizu, Y.; Sakaguchi, Y. J Text Machinery S Jpn 1999, 52, 274.
26. Stark, S. M., Jr.; Rowrand, S. P. J Appl Polym Sci 1966, 10, 1777.
27. Rowland, S. P., Post, A. W. J Appl Polym Sci 1966, 10, 1751.
28. Payet, G. L. Text Res J 1973, 43, 194.
29. Abe, S.; Ohta, S.; Yoshikawa, M.; Tsutsumi, M. J Text Machinery S Jpn 1999, 52, 65.
30. Fujishiro, H.; Ikebe, M.; Naito, T.; Noto, K. Cryog Eng 1993, 28, 533.
31. Wada, M.; Heux, L.; Isogai, A.; Nishiyama, Y.; Chanzy, H.; Sugiyama, J. Macromolecules 2001, 34, 1237.
32. Miyake, H.; Nagura, M. Text Res J 2001, 71, 645.
33. VanderHart, D. L.; Atalla, R. H. Macromolecules 1984, 17, 1465.
34. Horii, F. In Nuclear Magnetic Reasonance in Agriculture; Pfeffer, P. E.; Gerasimowicz, W. V., Eds.; CRC Press: Boca Ration, Florida, 1989; Ch. 10, p 311.
35. Dudley, R. L.; Fyfe, C. A.; Stephenson, P. J.; Deslandes, Y.; Hamer, G. K.; Marchessaulft, R. H. J Am Chem Soc 1983, 105, 2469.
36. Horii, F.; Hirai, A.; Kitamaru, R. Polym Bull 1982, 8, 163.
37. Horii, F.; Hirai, A.; Kitamaru, R. Macromolecules 1987, 20, 2117.
38. Yamato, H.; Horii, F.; Odani, H. Macromolecules 1989, 22, 4130.
39. Abe, S.; Ohta, S.; Yamanaka, A.; Nagara, N. J Text Machinery S Jpn 1996, 49, 290.
40. Hatakeyama, H.; Hatakeyama, T. Thermochim Acta 1998, 308, 3.
41. Woodcock, C.; Sarko, A. Macromolecules 1980, 13, 1183.
42. Ishikawa, A.; Sugiyama, J.; Okano, T. Wood Research 1994, 81, 16.
43. Earl, W. L.; VanderHart, D. L. Macromolecules 1981, 14, 570.
44. Kroschwitz, J. I. Concise Encyclopedia of Polymer Science and Engineering; Wiley: New York, 1990.
45. Abe, S.; Ohta, S.; Tsutsumi, M. J Text Machinery S Jpn 1997, 50, 109.
46. Guthrie, J. D. Text Res J 1967, 37, 40.
47. Heinisch, K.; Katayama, A.; Rouette, H. K.; Wehner, A.; Zollinger, H. Text Chem Color 1970, 2, 391.
48. Nomura, R.; Yoneyama, K.; Ogasawara, F.; Ueno, M.; Okuda, Y.; Yamanaka, A. Jpn J Appl Phys 2003, 42, 5205.
49. Hatakeyama, T.; Nakamura, K.; Hatakeyama, H. Polymer 1982, 23, 1801.